HEFAT2007
5th International Conference on Heat Transfer, Fluid Mechanics and Thermodynamics
Sun City, South Africa
Paper number: CR2

EXPERIMENTAL STUDY OF ULTRASONIC SIGNALS CHARACTERISTICS IN AIR-WATER BUBBLY FLOWS

Carvalho R .D. M.*[,1], Venturini O. J.[1], Neves-Jr. F.[2], Arruda, L. V. R.[2], and França, F. A.[3]
*Author for correspondence
[1]Universidade Federal de Itajubá (UNIFEI), Brazil, E-mail: martins@unifei.edu.br
[2]Universidade Tecnológica Federal do Paraná (UTFPR), Brazil
[3]Universidade Estadual de Campinas (UNICAMP), Brazil

ABSTRACT

In the oil industry there is a need to determine the dispersed phase holdup in multiphase flows using noninvasive, fast responding techniques; ultrasonic techniques apparently can fulfill these requirements. In this regard, the proposed paper analyzes the ultrasonic signals obtained through vertical, upward air-water flows in the zero to 14% void fraction range. Initially, the experimental apparatus and the flow patterns observed are discussed. Next follows a discussion of the ultrasonic signals characteristics and the trends in the transit time and attenuation. A new transit time definition is proposed that could be used for the characterization of two-phase flows.

INTRODUCTION

Multiphase flows are very common in the petroleum, chemical, and nuclear industries, oftentimes involving harsh media, strict safety restrictions, access difficulties, long distances, and aggressive surroundings. Accordingly, there is a growing interest in non-invasive techniques for measurement of the dispersed phases concentration in multiphase flows. Ultrasonic signals are information rich and the ultrasonic technique apparently can fulfill the requirements of remote sensing, long distance signal transmission, and harsh operating conditions. The main ultrasonic parameters normally used in process monitoring, measurement, and control are the signal amplitude and the wave transit time [1]. In multiphase flows, as the concentration and size distribution of the dispersed media (solid particles and/or gas bubbles) change these signal properties vary due to the combined effect of acoustic attenuation and transmission phenomena.

The ultrasonic technique has been used for the characterization of flow patterns of horizontal air-water two-phase flows and for the measurement of the liquid film thickness in horizontal air-mercury flows [2]. The authors presented and discussed the general features of the waveforms obtained; signal processing for computation of the void fraction was not discussed. The ultrasonic technique has also been used to measure the dispersed phases void fractions in three-phase and two-phase flows (air-oil; glass beads-oil; and air-glass beads-oil) [3,4]. Investigators in [3] observed the signal attenuation to increase exponentially with increasing interfacial area of both the solid and gas phases. The air bubbles were said to have caused an increase in the acoustic wave transit time. Besides confirming the observations in [3], investigators in [4] also verified that the scatter in the transit time and in the signal amplitude increased as the gas holdup increased.

Despite the growing number of papers dealing with the application of the ultrasonic technique for measurements in two-phase flows, to the present authors´ knowledge a detailed discussion of the signal waveforms and how they relate to the computation of the acoustic parameters does not seem to exist. Of immediate interest to the present study, data for the wave transit time are presented in the literature without a clear definition of this parameter [1,2,3,4]. For instance, a plot in [2] implies that the transit time is the time difference between the crests of isolated peaks associated with a single pulse emission and reception at the top and bottom transducers placed on the outer surface of the horizontal pipe.

However, digital data acquisition and processing equipment have undergone enormous improvements in the past decade; better resolution, higher sampling frequency, and larger storage capacity allow for new information on the acoustic pulse interaction with dispersed mixtures to be readily obtained using fairly inexpensive hardware. From this standpoint, the present paper is intended mainly as a contribution to a better understanding of the acoustic wave transit time and its potential for characterization of multiphase flows. More specifically, the present work tries to identify the acoustic phenomena imprinted in the waveforms and discusses the computation of the wave attenuation and transit time from the raw, digitized ultrasonic signals across bubbly air-water flows.

EXPERIMENTAL APPARATUS AND PROCEDURE

Two-Phase Flow Test Rig

An experimental apparatus was designed and built specifically for the study of the ultrasonic measurement of the void fraction in vertical, upward air-water flows (Figure 1). The air-water mixer consists of a water-filled tank where the lower

end of a 54-mm inner diameter acrylic pipe is inserted. Inside this pipe there is a cylindrical porous medium through which compressed air is injected into the water flow; mixing of the air and water takes place in the annular space so formed and rapidly evolves into the bubbly flow pattern. Downstream of the mixer, a 3.5-m long section of the acrylic pipe assures the hydrodynamic development of the bubbly flow before it enters the ultrasonic probes test section. This test section is actually a 10-cm long segment of the same 54-mm diameter acrylic pipe where the ultrasonic probes are attached. In addition, a variable reluctance pressure transducer tapped just downstream of the ultrasonic probes measures the flow pressure; this reading is necessary for the calculation of the air flow rate under actual test conditions. Following the test section, a 1.6-m long portion of the acrylic pipe discharges the air-water two-phase flow into a phase separator. A quick valve device installed in this part of the flow loop allows for measurements of the volumetric void fraction. This measurement system replaced a previously installed double needle conductive probe [5]; results from both systems can be used to corroborate the measurements made with the ultrasonic probes.

In the separator the air is vented into the atmosphere while the gravity driven water flow returns to the liquid reservoir. A centrifugal pump then forces the water back to the air-water mixer, thus closing the flow loop. A heat exchanger located downstream of the pump is used to restrain variations in the water temperature; the cooling stream is running water at ambient temperature. A variable speed driver allows for a zero to 5,000 kg/hr water flow rate variation. The water flow rate is measured by Rheonik RHM12 Coriolis-type flow meter, which includes an RTD for temperature measurements. The air flow rate is measured by 50MJ10-9 and 50MJ10-12 Meriam Instruments laminar flow elements. Model PX 750 Omega pressure transducers, ranging from 0 to 700 mmH_2O, are used to measure the pressure difference across the laminar flow elements. An identical transducer, tapped downstream the laminar flow elements, reads the gage air flow pressure. Atmospheric pressure measurements come from the University weather station, reported continuously through Internet. A type J thermocouple measures the flowing air temperature. Bourdon type and U manometers and digital display thermocouples allow for double checks on these automatic digital measurements as well as direct visual monitoring of the flow loop proper operation. Values of the operating parameters are then entered into a Microsoft Excel spreadsheet that calculates the actual air flow rate at the test section and the air and water superficial velocities. A filming station downstream of the test section allows for high speed motion pictures (1000 fps) of the two-phase flow.

Ultrasound Instrumentation

Figure 2 shows a schematic view of the test section instrumentation. Two plexiglass adapters, 40-mm and 10-mm long, were curved machined on one side so as to be snugly fitted to the outer surface of the plexiglass pipe. Panametrics emitter and receiver ultrasonic transducers were then fixed to the opposite surfaces of the 40-mm and 10-m adapters, respectively; for the particular emitter transducer used this

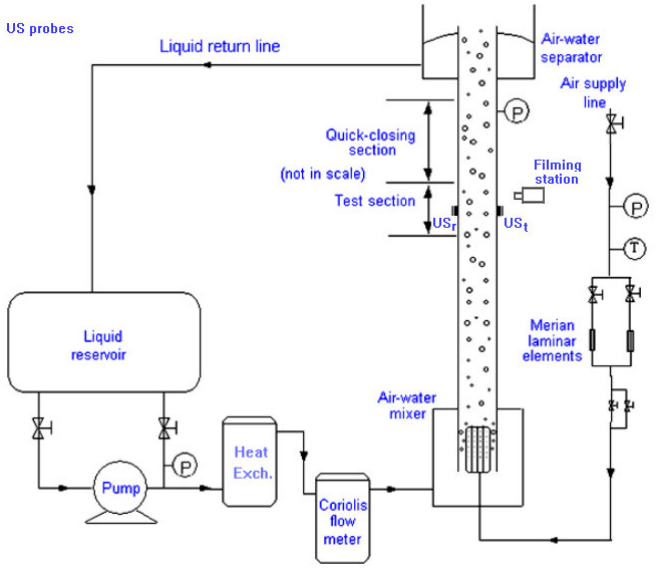

Figure 1 Schematic view of the air-water bubbly flow test rig.

ensures locating the acoustic near field in the 40-m plexiglass block and not in the two-phase flow [6]. A thin gel layer was applied to the transducers front surface before mounting to enhance mechanical contact. The emitter-receiver ultrasonic path is then made of a 40-mm long distance across the acrylic block on the emitter side, a 3-mm long crossing of the acrylic pipe wall, the 54-mm crossing of the two-phase mixture inside the pipe, and a 10-mm long distance across the acrylic block on the receiver side. In the wave transit time calculations, the gel layer thickness was neglected.

A three-channel, USB 2.0 computer connected electronic board was designed and built specifically for this research project. This stand-alone board consists of an ultrasound pulse emitter and a data acquisition system with a 20MHz maximum sampling frequency and 32Mb storage capacity. Thus, the sampling time could be extended far beyond what is allowed even by sophisticated commercial equipment. This was necessary to completely capture the axial distribution of the two-phase structures under study. This board was used for data acquisition, storage, and preliminary reduction.

Experimental Procedure

In this research project [7,8] the trends in the experimental data were as expected; the signal amplitude and energy ratios decreased exponentially as the void fraction increased. Yet, the scatter in the data was large and every effort was now made to reduce it. The following measures were taken**:**

1. According to a preliminary statistical analysis [8], ten ultrasonic samples were obtained for each test condition. Given an appropriate sampling period, this should be enough to reduce the scatter in the data without making the experimentation too cumbersome.
2. The sampling period was set to 1.75 sec in order to catch the various structures making up the typical axial bubbly flow topology for the conditions tested. Therefore, no discrepancy should arise for the same test condition due to a limited number of gas structures being sampled.

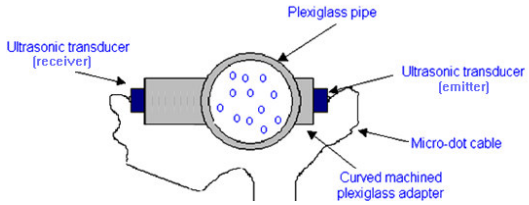

Figure 2 Schematic view of ultrasonic instrumentation assembly.

3. The acquisition board works at 20MHz allowing for 32 Mb to be stored during 1.75 sec. The ultrasound transducer is excited at 4.1 kHz, which corresponds to 7168 received pulses during the sampling period.
4. The water flow rate was kept constant while the air flow rate was varied so as to give the desired void fraction values. Hence, the flow displacement during each sampling interval was the same and so was the portion of the gas phase axial distribution sampled.
5. The water in the test rig was forced to flow through a heat exchanger cooled by running water at ambient temperature, which reduced temperature variations during test runs.
6. The single-phase still water signals used as reference in the calculations of the amplitude and energy ratios were selected so as to match as closely as possible the flow temperature corresponding to the two-phase signals. This should minimize any discrepancies arising from the effect of temperature on signal attenuation.

Ultrasonic data were then obtained for the entire bubbly flow regime, i.e. zero to 14% void fraction range, in 1% steps. In addition, for each void fraction value the two-phase flow was filmed at 250 fps. The ultrasonic wave amplitude and energy attenuation as well as the transit time were then calculated by an independent MatLab signal processing algorithm. Independent measurements of the radial distribution and mean values of the void fraction, bubble diameter, bubble frequency, bubble velocity, and interfacial area density, as reported in [5] for the same operating conditions, are available for reference.

BUBBLY FLOW SUB-REGIMES

The two-phase flow films were analyzed so as to identify different flow patterns as the void fraction increased within the so-called bubbly flow regime. In this way, it would be possible to systematically relate changes in the ultrasonic signal responses to different two-phase flow structures. In the present paper, only the flow patterns main characteristics and their implications on the acoustic parameters will be discussed.

From visual comparisons of the gas phase forms and distributions, the bubbly flow sub-regimes below were identified. For $\alpha \leq 8\%$, the visual observations are supported by measurements in [5] for the same flow conditions.

Discrete bubbles sub-regime ($\alpha \leq 3\%$) — the bubbles density population increases gradually, bubble size is from small to medium, and bubble distribution is essentially uniform both radially and axially (Figure 3).

Discrete bubbles and gas clots sub-regime ($3 < \alpha \leq 8\%$) — similar to the previous sub-regime except that small, mushroom-shaped gas clots are now present (Figure 4). In addition, there seems to exist axially alternated regions of relatively low and high bubbles density population.

Cap bubbles sub-regime ($8 < \alpha \leq 12\%$) — slug shaped gas clots or cap bubbles begin to appear; they are narrower than the pipe diameter and do not occur frequently. The flow, however, is more agitated and regions of high and low bubble density become more distinct (Figure 5).

From 12% on, the slug flow regime seems to be firmly established; clearly shaped, massive slugs are observed (Figure 6). They occur very regularly and in their wake alternated regions of high and low void fractions are easily distinguished.

ULTRASONIC SIGNALS CHARACTERISTICS

Figure 7 shows a typical trace signal from the present ultrasound emitter-receiver assembly. The "bang" is actually a noise related, emitted pulse markup. The first incoming pulse hits the ultrasound receiver as a longitudinal wave attenuated by and transmitted through the air-water bubbly mixture and plexiglass elements. The second incoming pulse is a small-scale version of the first one and is due to the shear wave generated at the curved pipe wall [7]; it travels at a lower velocity and thus hits the receiver transducer some time after the longitudinal wave. The ultrasonic data collected also showed that the first valley in the first incoming pulse was much more sensitive to void fraction variations than the first peak in the same sequence. The amplitude of the received signal was then somewhat arbitrarily taken as that of the first valley immediately following the signal arrival; mathematically it is identified as an inflection point [7].

As shown in Figure 8, the acoustic pulses waveform changed throughout the bubbly flow regime; the peaks and valleys were smoothed out gradually, evidencing an increasing obstruction of the acoustic path. On the other hand, the pulse duration (the time interval between the moment the wave first hits the receiver and the moment it dies out) remained almost constant. A spectral analysis was then carried out, which, as expected, showed no significant differences between the emitted and received pulses frequency composition. In order to get new insights into the mechanisms whereby the two-phase flow hinders acoustic energy transmission, attention was focused on the wave transit time. This is discussed next.

ENERGY WEIGHTED WAVE TRANSIT TIME

The initial transit time and the pulse duration remained essentially constant (Figure 8), which supports the assumption that gas bubbles have no effect on sound velocity [4]. Nonetheless, a new definition of the wave transit time was tried to reveal whether different mechanisms of acoustic attenuation come into play as the void fraction increases.

$$\Delta t_{total} = \Delta t_{initial} + \frac{\int_{E_1}^{E_2} t \, dE}{E_{total}} \qquad (1)$$

In the equation above, $\Delta t_{initial}$ represents simply the definition of transit time in [7], that is, the instant of time when the acoustic longitudinal wave first hits the receiver. It then implies minimum or no disturbance of the acoustic beam by the bubbles. The second term is the pulse mean transit time interval weighted by the amount of energy that gets to the receiver at each infinitesimal time increment; it can be interpreted as a bulk measure of the effect of flow topology and mean void fraction on the phase of the received signals.

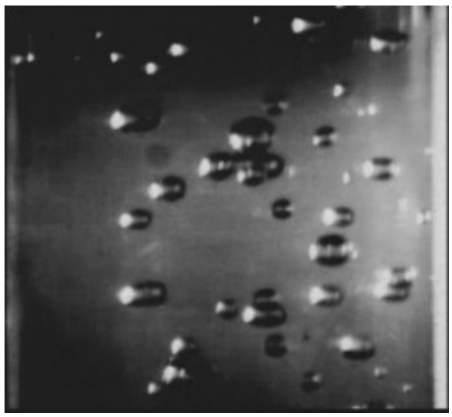

Figure 3: Discrete bubbles sub-regime (α = 1%).

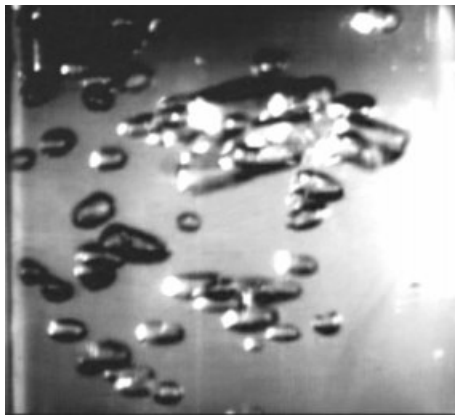

Figure 4: Discrete bubbles and gas clots sub-regime (α = 5%).

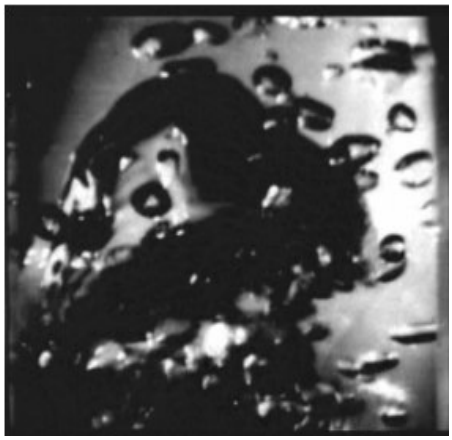

Figure 5: Cap bubbles sub-regime (α = 11%).

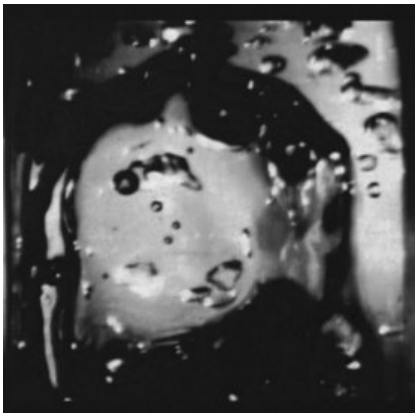

Figure 6: Typical overall view of the slug flow (α = 13%).

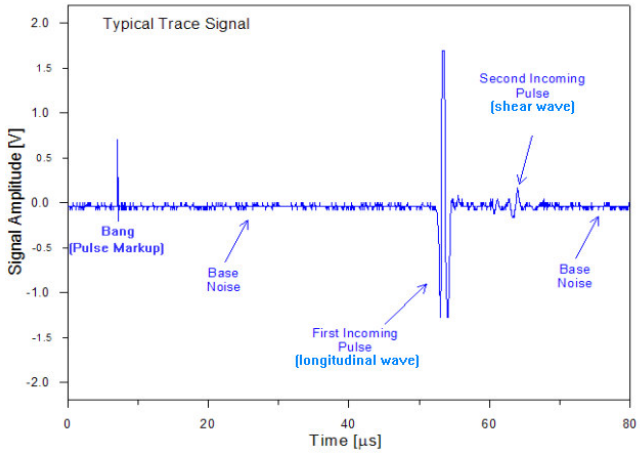

Figure 7: Trace signal of the ultrasonic emitter-receiver assembly.

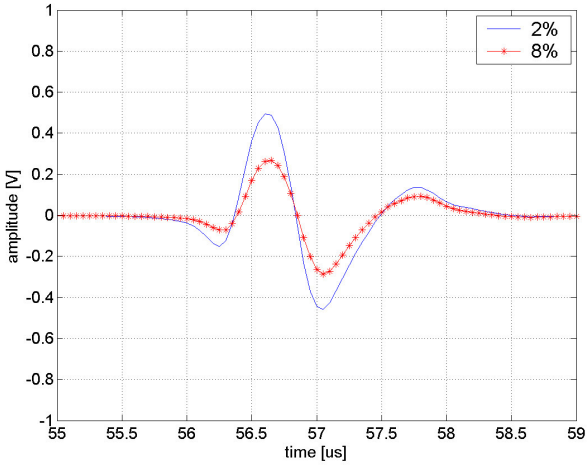

Figure 8: Average response signals for α = 2% and α = 8% (approximately 7,168 pulses for each condition).

Figure 9 shows Δt_{total} and $\Delta t_{initial}$ as a function of the void fraction. It can be seen that $\Delta t_{initial}$ exhibited only a very slight increase (less than 1 µsec) throughout the entire bubbly flow regime. This is consistent with the assumption that

$\Delta t_{initial}$ is associated with the fraction of the acoustic energy that gets to the receiver transducer with minimum or no disturbance by the bubbles, thus representing mainly transmission through the continuous phase. From this point of view, the results for $\Delta t_{initial}$ support the claim by many investigators [4] that the speed of sound is independent of gas holdup due to the great distortion of ultrasound around bubbles. As to Δt_{total}, it exhibited a 1-μsec variation throughout the void fraction range tested. Since each data point represents an average value calculated from ten samples for each condition, each sample containing about 7,000 pulses, the 1-μsec variation cannot be simply dismissed as data scatter. A better understanding of this behavior can be gained from Figure 10, which displays the integral term in the right-hand side of Equation (1) as a function of the void fraction. Not surprisingly, the same behavior observed for Δt_{total} is observed here. From 0 to 3% void fraction (discrete bubbles sub-regime), the pulse mean transit time decreased whereas from 3% to 6% (discrete bubbles and gas clots sub-regime) it remained essentially constant. From 6% on (cap bubbles sub-regime and slug flow), it steadily increased. This behavior results from the complex interplay between the medium, the emitted pulse characteristics and the receiving sensor dynamics. Bubbles and larger gas structures can cause scattering, dispersion, or even a direct blockage of the acoustic beam; absorption, reflection, refraction, and forward scattering can all come into play in an overall measurement of acoustic attenuation.

In the discrete bubbles sub-regime, the weighted transit time decreased as the void fraction increased. Even though forward scattering contributions are usually small, significant increases in the total energy incident on the receiver transducer due to forward scattering are possible [9]. Thus, it is conceivable that the positive contribution of forward scattering would prevail upon the negative contributions of attenuation and reflection, causing a decrease in the weighted transit time. In addition, investigators in [10] reported a slight increase in the measured peak value of response signals of spheres (simulating bubbles) in line along the ultrasonic path as compared to the value calculated considering the spheres to be perfect reflectors of the incident wave. The authors claimed the increase was due to multiple reflections from the ultrasonic beam side lobes. The present investigators believe a similar mechanism could also contribute to a more effective transmission of the ultrasonic energy in the discrete bubbles sub-regime.

In the discrete bubbles and clots sub-regime, the weighted transit time remained essentially constant. Subsequently, in the cap bubbles sub-regime and in the slug flow it steadily increased; most likely attenuation by and, mainly, reflection off large gas structures increasingly hinder and divert the acoustic energy. Finally, the pulse weighted transit time (Figure 10) is substantially higher than the pulse duration. Whereas the latter refers to a chronological time frame, the former is rather a measure of the interaction between the acoustic wave and the gas phase structures. As such, the pulse mean transit time and Δt_{total} in Equation (1) are not intended to be used in ultrasonic measurement methods based on transit time variations; their purpose is mainly to provide a concise means to characterize the two-phase flow.

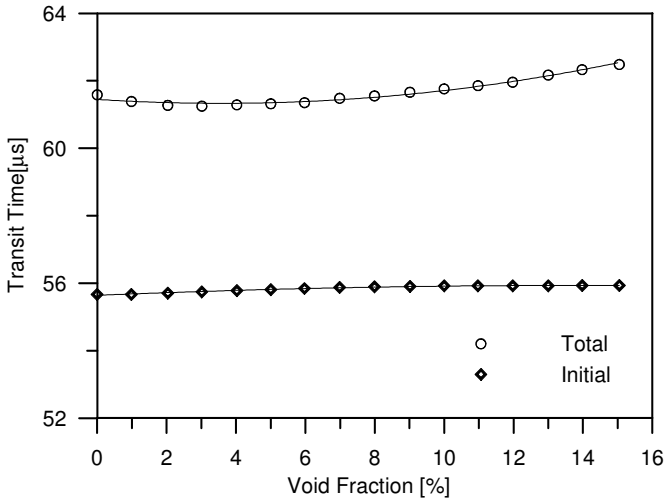

Figure 9: $\Delta t_{initial}$ and Δt_{total} as a function of void fraction.

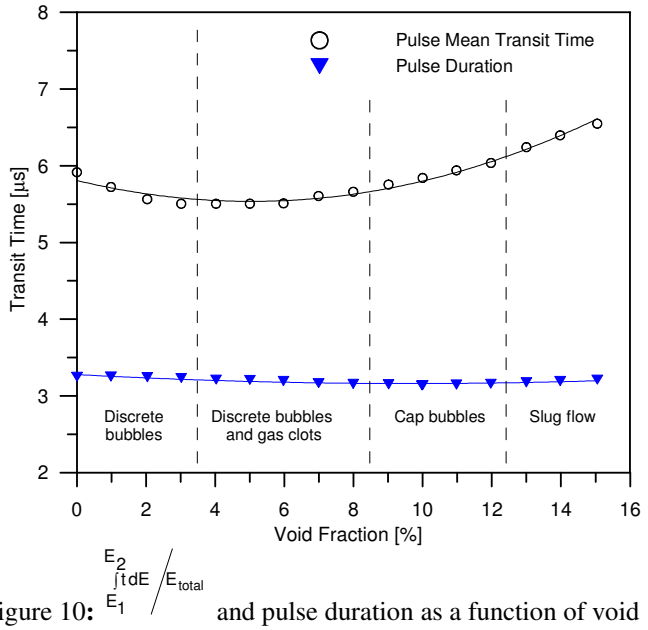

Figure 10: $\int_{E_1}^{E_2} t\,dE \Big/ E_{total}$ and pulse duration as a function of void fraction.

RESPONSE SIGNALS ATTENUATION

Ultrasonic data were collected in the zero to 15% void fraction range. The average amplitude and energy ratios decrease with increasing void fraction (Figure 11). Moreover, except for the transition from the discrete bubbles and gas clots sub-regime to the cap bubbles sub-regime, there are clear changes in slope that match very closely the bubbly flow sub-regimes discussed previously. These results indicate that the ultrasound is indeed able to capture changes in flow pattern.

Figure 12 displays the average energy ratios as a function of the void fraction and interfacial area density. The plot shows that a 15-fold increase in the void fraction corresponds to a ten-fold increase in the interfacial area density as the air flow rate was stepped up for the given water flow rate. On the other

hand, the functional dependence of the energy ratio on either the void fraction or the interfacial area density is very similar. Hence, the void fraction is a more appropriate parameter to describe the two-phase flow conditions due to its higher sensitivity and more readily calculation.

Figure 11 e Figure 12 also show that the measures discussed previously to reduce data scatter were very effective.

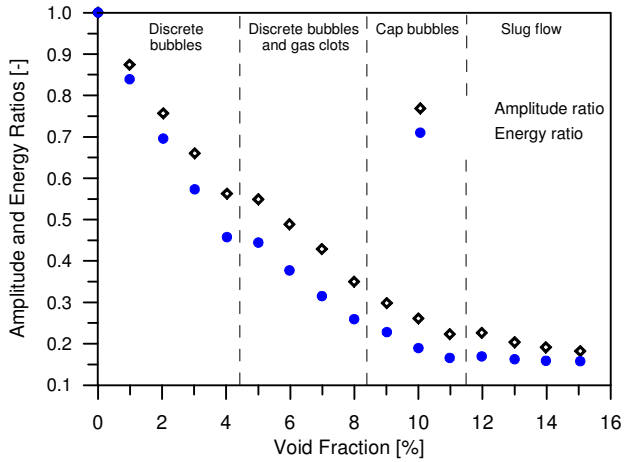

Figure 11: Average amplitude and energy ratios as a function of void fraction (j_{water} = 25,5 cm/s).

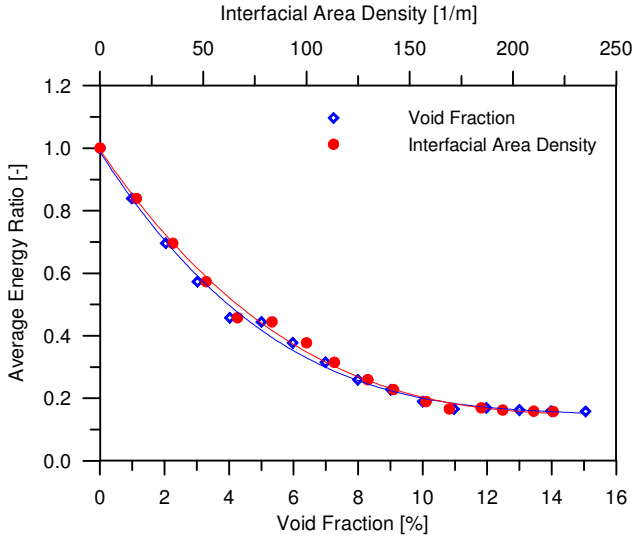

Figure 12: Average energy ratios as a function of void fraction and interfacial area density (j_{water} = 25,5 cm/s).

CONCLUSION

An experimental apparatus was designed and built for the ultrasonic measurement of the void fraction in vertical, upward air-water flows. Ultrasonic data were then obtained for the zero to 14% void fraction range, in 1% steps; in addition, for each void fraction value the two-phase flow was filmed at 250 fps. Three bubbly flow sub-regimes were then identified, namely, discrete bubbles ($\alpha \leq 3\%$), discrete bubbles and gas clots ($3 < \alpha \leq 8\%$), and cap bubbles ($8 < \alpha \leq 12\%$). From 12% on, the slug flow regime seems to be firmly established. Based on a systematic study of the ultrasonic signals, a new definition of the acoustic wave transit time was proposed. This new definition is not intended to be used in measurement methods based on transit time variations; its main purpose is to provide a concise means to characterize the two-phase flow topology. The average amplitude and energy ratios decreased with void fraction and exhibited changes in slope that matched the bubbly flow sub-regimes transitions. This indicates the ultrasound is able to capture changes in flow pattern. Finally, measures were taken that greatly reduced the scatter in the acoustic data.

ACKNOWLEDGEMENTS

The authors acknowledge the financial support received from PETROBRÁS, the *Brazilian National Petroleum Company*, which made possible this study.

REFERENCES

1. Bond, L. J., Morra, M., Greenwood, M. S., Bamberger, J. A., Pappas, R. A., Ultrasonic Technologies for Advanced Process Monitoring, Measurement, and Control. In: *Proceedings 20th IEEE Instrumentation and Measurement Technology Conference*, Vail, CO, USA, 2003.
2. Chang, J. S., Ichikawa, Y., Irons, G. A., Flow Regime Characterization and Liquid Film Thickness Measurment in Horizontal Gas-Liquid Two-Phase Flow by an Ultrasonic Method. In: *AIAA/ASME Joint Plasma Thermophysics HTC*, 1982.
3. Zheng, Y., Zhang, Q., Simultaneous Measurement of Gas and Solid Holdups in Multiphase Systems Using Ultrasonic Technique. *Chemical Engineering Science*, Vol. 59, pp. 3505-3514, 2004.
4. Vatanakul, M., Zheng, Y., Couturier, M., Application of Ultrasonic Technique in Multiphase Flow. *Industrial and Engineering Chemistry Research*., Vol. 43, pp. 5681-5691, 2004.
5. Dias, S., França, F. A., Rosa, E. S., Statistical Method to Calculate Local Interfacial Variables in Two-Phase Bubbly Flows Using Intrusive Crossing Probes. *International Journal of Multiphase Flow*, Vol. 26, No. 11, pp. 1797-1830, 2000.
6. PANAMETRICS, *Technical Notes*, p. 40, 2005.
7. Vasconcelos, A. M., Carvalho, R. D. M., Venturini, O. J., França, F. A., The Use of the Ultrasonic Technique for Void Fraction Measurements in Air-Water Bubbly Flows. In: *Proceedings of the 11th Brazilian Congress of Thermal Sciences and Engineering*, Curitiba, Brazil, 2006.
8. Carvalho, R. D. M., Venturini, O. J. Neves Jr., F., and França, F. A., Analysis of Ultrasonic Signals Used for the Characterization of Bubbly Air-Water Two-Phase Flows, *Proceedings of the IV Congresso Rio Automação*, 2007.
9. Jones, S. W., Amblard, A., and Favreau, C., 1986, *Interaction of an Ultrasonic Wave with a Bubbly Mixture, Experiments in Fluids*, Vol. 4, pp. 341-349.
10. Xu, L. A., Green, R. G., Plaskowski, A., and Beck, M. S., The pulsed ultrasonic cross-correlation flowmeter for two-phase flow measurement, *J. Phys. E: Sci. Instrum.*, Vol. 21, 1988, pp. 406-414.